JACS
JOURNAL OF THE AMERICAN CHEMICAL SOCIETY
Communication
pubs.acs.org/JACS

$Mg(PF_6)_2$-Based Electrolyte Systems: Understanding Electrolyte–Electrode Interactions for the Development of Mg-Ion Batteries

Evan N. Keyzer,[†] Hugh F. J. Glass,[†,§] Zigeng Liu,[†] Paul M. Bayley,[†] Siân E. Dutton,[§] Clare P. Grey,*[,†] and Dominic S. Wright*[,†]

[†]Department of Chemistry, University of Cambridge, Lensfield Road, Cambridge CB2 1EW, U.K.
[§]Cavendish Laboratory, Department of Physics, University of Cambridge, JJ Thomson Avenue, Cambridge CB3 0HE, U.K.

Supporting Information

ABSTRACT: $Mg(PF_6)_2$-based electrolytes for Mg-ion batteries have not received the same attention as the analogous $LiPF_6$-based electrolytes used in most Li-ion cells owing to the perception that the PF_6^- anion decomposes on and passivates Mg electrodes. No synthesis of the $Mg(PF_6)_2$ salt has been reported, nor have its solutions been studied electrochemically. Here, we report the synthesis of the complex $Mg(PF_6)_2(CH_3CN)_6$ and its solution-state electrochemistry. Solutions of $Mg(PF_6)_2(CH_3CN)_6$ in CH_3CN and CH_3CN/THF mixtures exhibit high conductivities (up to 28 $mS{\cdot}cm^{-1}$) and electrochemical stability up to at least 4 V vs Mg on Al electrodes. Contrary to established perceptions, Mg electrodes are observed to remain electrochemically active when cycled in the presence of these $Mg(PF_6)_2$-based electrolytes, with no fluoride (i.e., MgF_2) formed on the Mg surface. Stainless steel electrodes are found to corrode when cycled in the presence of $Mg(PF_6)_2$ solutions, but Al electrodes are passivated. The electrolytes have been used in a prototype Mg battery with a Mg anode and Chevrel (Mo_3S_4)-phase cathode.

The development of the rechargeable lithium-ion battery has facilitated the production of many current portable devices such as mobile phones, laptop computers, and digital cameras, revolutionizing global communication.[1] Nonetheless, Li-ion battery technology still faces many challenges, including the need to increase the batteries' energy density. Magnesium-ion batteries have been proposed as safer, cheaper, and potentially higher capacity alternatives to Li-based systems, with a theoretical anode capacity for Mg of 3833 $mAh{\cdot}cm^{-3}$, nearly twice that of Li metal systems (2062 $mAh{\cdot}cm^{-3}$) owing to the two valence electrons carried by magnesium.[2] Mg-ion battery chemistry in principle permits the use of highly earth-abundant Mg metal as an anode material without the potential risk of thermal runaway resulting from dendrite formation that can occur when using Li metal anodes.[3] However, a major limiting factor in developing competitive Mg-ion batteries is the lack of an electrolyte that is stable over a wide voltage range and compatible with multiple positive and negative electrode materials.[4] Established high-voltage electrolytes, such as the magnesium aluminum chloride complex (MACC) in THF and $Mg(TFSI)_2$ in glymes, which are stable to at least 3.4 V vs Mg, are known to corrode common stainless steel battery components and exhibit only moderate ionic conductivities.[5]

Many Li electrolyte systems have been developed and studied using a wide range of Li salts, including $LiBF_4$, $LiClO_4$, LiTFSI, $LiPF_6$, $LiAsF_6$, and $LiSbF_6$.[6] Due to a balance of several properties that no other common Li salt has been found to possess, $LiPF_6$ ultimately became the preferred electrolyte and was commercialized by Sony Corp. in 1991.[7] Despite the thermal and hydrolytic instability of the PF_6^- anion, $LiPF_6$ has been found to be highly electrochemically stable in mixed carbonate solvents, allowing for the construction of Li-ion batteries with cathode operating potentials of 4.6 V vs Li.[8] Further, $LiPF_6$-carbonate solutions are highly ionically conductive electrolytes. Due to the relatively labile P–F bonds, PF_6^--based electrolytes are able to form passivating layers on various electrodes and commonly used aluminum current collectors, thereby inhibiting continuous breakdown of the electrolyte during battery cycling and corrosion of the current collector, helping to prevent device failure.[9]

Despite the ubiquity of $LiPF_6$ in Li-ion systems, $Mg(PF_6)_2$ has not received the same attention, and to the best of our knowledge, no direct synthesis of $Mg(PF_6)_2$ compounds has been reported. It is generally thought that the PF_6^- anion decomposes on Mg anodes, forming passivating MgF_2 layers.[10] However, no detailed study of the electrochemistry or potential passivating or corrosive nature of $Mg(PF_6)_2$ has been conducted to date. Here, we report the synthesis and characterization of a Lewis base complex of $Mg(PF_6)_2$, $Mg(PF_6)_2(CH_3CN)_6$ (**1**), as well as the plating and stripping of Mg/Mg^{2+} employing **1**-based electrolytes using glassy carbon (GC) and Mg electrodes. We also demonstrate the use of a $Mg(PF_6)_2$-based electrolyte in a Mg-ion battery using a Mg anode.

We note that the synthesis of $Ca(PF_6)_2$ via a metathesis route has been reported.[11] However, as this method often leads to high levels of impurities that are difficult to remove, it has not been attempted in this study.[12] Instead, $Mg(PF_6)_2$ was prepared using $NOPF_6$ and Mg metal, according to procedures used for the formation of transition metal tetrafluoroborate and hexafluorophosphate complexes.[13] Mg metal, activated with a small amount of I_2 in dry CH_3CN, was treated with a solution of $NOPF_6$ in dry CH_3CN at room temperature under an atmosphere of N_2. As the reaction mixture was stirred, the

Received: April 27, 2016
Published: June 30, 2016

DOI: 10.1021/jacs.6b04319
J. Am. Chem. Soc. 2016, 138, 8682–8685

solution evolved a colorless gas (NO); after stirring for 1 h at room temperature the solution was heated to 45 °C for 20 h (eq 1). After removal of solvent, the off-white solid was recrystallized

$$Mg + 2NOPF_6 \xrightarrow[45\ ^\circ C,\ 20\ h]{CH_3CN} \underset{(\mathbf{1})}{Mg(PF_6)_2(CH_3CN)_6} + 2NO_{(g)} \quad (1)$$

twice from hot acetonitrile, affording a highly pure white crystalline powder of $Mg(PF_6)_2(CH_3CN)_6$ (**1**) in a 52% yield (product being lost during the two recrystallization steps).

The ^{19}F and ^{31}P NMR spectra of **1** exhibit a doublet and heptet, respectively, characteristic of the PF_6^- anion. X-ray analysis of a single crystal obtained from the diffusion of Et_2O into a CH_3CN solution of **1** shows the complex to be $Mg(PF_6)_2(CH_3CN)_6$ (Figure 1). Bulk purity of **1** was confirmed by elemental analysis (C, H, and N). The IR spectrum of **1** exhibits the expected C≡N stretching band at 2299 cm^{-1}.

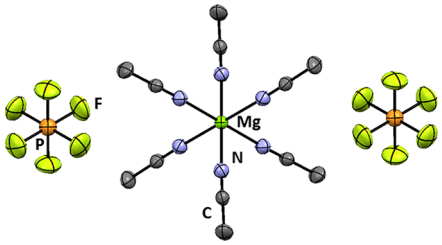

Figure 1. X-ray crystal structure of **1**, displaying thermal ellipsoids at 50% probability. Protons and anion disorder have been omitted for clarity (Mg, green; P, orange; F, yellow; N, blue; C, gray).

Complex **1** could be dissolved in CH_3CN to a maximum concentration of 0.12 M at 25 °C. Interestingly, it was found to be significantly more soluble in a 1:1 mixture of THF/CH_3CN, reaching a maximum concentration of 0.71 M at 25 °C. The ionic conductivity of the 0.12 M electrolyte solution in CH_3CN is 18.7 $mS{\cdot}cm^{-1}$ at 25 °C, while those of the 0.12 and 0.71 M solutions in 1:1 THF/CH_3CN are 10.0 and 28.3 $mS{\cdot}cm^{-1}$, respectively. These conductivities are of the same order of magnitude as those reported for $LiPF_6$ in CH_3CN,[14] and significantly higher than those measured for MACC in THF (0.26 $mS{\cdot}cm^{-1}$, 0.04 M)[5a] and $Mg(TFSI)_2$ in 1:1 glyme/diglyme (5.22 $mS{\cdot}cm^{-1}$, 0.5 M).[5b] To gain insight into the structure of the electrolyte, spin−lattice, T_1 relaxation, and pulse field gradient diffusion NMR spectroscopic measurements were conducted on the various electrolytes (Supporting Information, Table S1 and Figure S6). The T_1 relaxation times of both the THF and CH_3CN protons in the 1:1 THF/CH_3CN solutions decrease in the presence of the Mg salt. The diffusion coefficients of the two molecules in the 0.71 M 1:1 THF/CH_3CN electrolyte solutions drop from 4.2 and 4.7, to 1.7 and 2.2 × 10^{-9} $m^2{\cdot}s^{-1}$, for THF and ACN, respectively, indicating strong interactions with Mg for both molecules.

Having successfully isolated a complex of $Mg(PF_6)_2$, we turned to its use as an electrolyte salt. A 1:1 THF/CH_3CN electrolyte solvent mixture was found to exhibit superior electrochemical stability and plating/stripping reversibility on GC compared to the 0.12 M electrolyte solution in pure CH_3CN under the same conditions. Cyclic voltammetry (CV) showed that a 0.12 M solution of **1** in 1:1 THF/CH_3CN could be cycled reversibly between −0.5 and 1.5 V vs Mg over at least 20 cycles at a rate of 25 $mV{\cdot}s^{-1}$ using a GC working electrode and Mg reference and counter electrodes (Figure 2a). The electrolyte

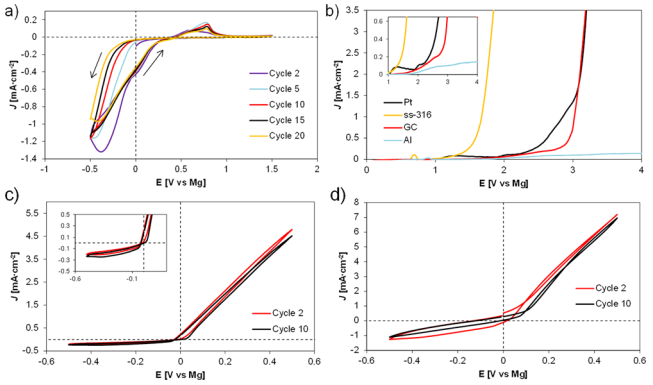

Figure 2. (a) Selected CV cycles of a 0.12 M solution of **1** in 1:1 THF/CH_3CN cycling at a rate of 25 $mV{\cdot}s^{-1}$ in a three-electrode cell containing a GC working electrode and Mg reference and counter electrodes. (b) LSV of 0.12 M **1** in 1:1 THF/CH_3CN, scanning at a rate of 25 $mV{\cdot}s^{-1}$ on Pt, ss-316, GC, and Al working electrodes (inset: expansion of region showing current density arising from the Al electrode). Selected CV cycles of (c) 0.12 M (inset: expansion of the region showing Mg plating) and (d) 0.71 M solutions of **1** in 1:1 THF/CH_3CN cycling at a rate of 50 $mV{\cdot}s^{-1}$ in a symmetric three-electrode Mg-flooded cell. All experiments were conducted at 25 °C.

could be cycled for at least 20 cycles with only moderate loss in plating/stripping current, exhibiting a small stripping overpotential (~0.25 V vs Mg) and a plating onset at 0 V vs Mg. The broad features observed around 0 V vs Mg on returning to positive potentials, thought to be the result of capacitive effects arising from the GC electrode, prevented the determination of meaningful cycling efficiency values.

As MgF_2 passivation on Mg electrodes resulting from $Mg(PF_6)_2$ decomposition is believed to hinder Mg plating/stripping, a symmetric flooded cell (Mg|Mg|Mg) using Mg as the working and counter electrodes was used to study these processes. Both the 0.12 and 0.71 M solutions of **1** in 1:1 THF/CH_3CN were cycled between −0.5 and 0.5 V vs Mg at a rate of 50 $mV{\cdot}s^{-1}$ for 10 cycles. CV of the 0.12 and 0.71 M electrolyte solutions exhibited little to no attenuation of current density, suggesting that the Mg electrode remains free of insulating films after cycling at potentials where Mg plating is expected (Figure 2c,d). That these anodic processes begin around 0 V vs Mg (i.e., with very small overpotentials) further suggests that Mg is removed directly from the metal surface, rather than through breakdown of a surface film followed by Mg removal.[10a] A higher current is observed in the more concentrated electrolyte, most likely reflecting its higher conductivity.

The electrochemical stability of the optimized $Mg(PF_6)_2$ electrolyte was further studied by performing linear sweep voltammetry (LSV) using Pt, GC, stainless steel (ss-316), and Al working electrodes (Figure 2b). On the Pt and GC electrodes, the onset of electrolyte oxidation begins with a minor anodic process around 2 V vs Mg, followed by more significant processes at 2.5 and 3 V vs Mg, respectively. On ss-316, oxidation occurs at much lower potentials of ~1.5 V vs Mg. Significantly, only very little current is observed when scanning with the Al working electrode out to 4 V vs Mg, suggesting that the Al surface is passivated toward the breakdown of the electrolyte. More extended LSV experiments of the 0.71 M solution again showed the onset of oxidation of the electrolyte to be significantly lower on ss-316 (ca. 2 V vs Mg) than Pt, GC, or Al. While significant current density was observed during the first sweep on ss-316,

DOI: 10.1021/jacs.6b04319
J. Am. Chem. Soc. 2016, 138, 8682−8685

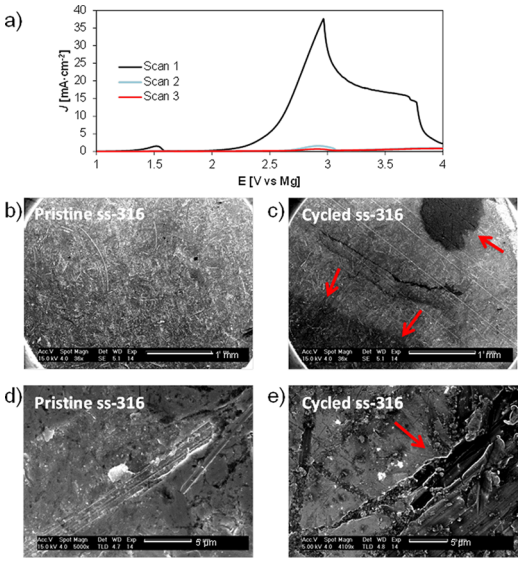

Figure 3. Corrosion of ss-316 electrodes cycled with a 0.71 M solution of **1** in 1:1 THF/CH_3CN. (a) Linear sweep voltammograms obtained at a rate of 25 mV·s^{-1} on a ss-316 working electrode. (b) SEM of the ss-316 current collector and (d) 5000× magnification. (c) SEM of the cycled ss-316 current collector showing large areas of corroded material, and (e) a 4109× magnification of the corroded area.

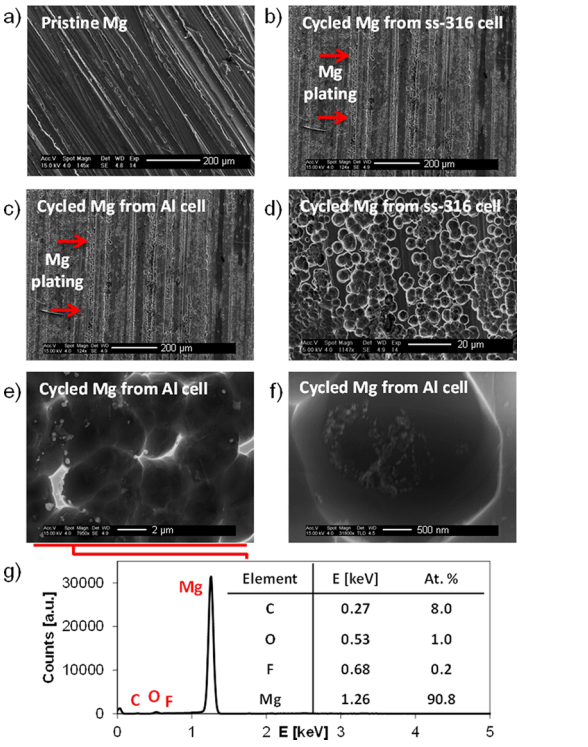

Figure 4. Surface analysis of pristine and Mg electrodes in 0.71 M **1** in 1:1 THF/CH_3CN. (a) SEM of an as-prepared Mg electrode. SEM of Mg electrodes taken from cycled cells containing (b) ss-316 and (c) Al current collectors, showing large areas of Mg deposition. SEM of a cycled Mg electrode taken from a cell containing (d) ss-316 and (e) Al current collectors, highlighting the globular Mg plating morphology. (f) SEM of a single Mg bead deposited on the surface of a Mg electrode cycled with Al current collectors. (g) EDX analysis of the deposited Mg beads shown in (e).

subsequent sweeps showed very little current density up to 4 V vs Mg (Figure 3a), the attenuation of current suggesting that the electrolyte reacts with the surface of the ss-316 electrode to form an insulating film.

More extended cycling results with the 0.71 M electrolyte (see Figures S8–S11) performed on Mg symmetric cells using either ss-316 or Al current collectors and a current of 5 mA·cm^{-2} show that the overpotential for both stripping and plating grows steadily over the first 10 h to ~0.6 V (on both electrodes), thereafter dropping to a steady-state value of 0.5 V, the overpotential remaining constant for more than 250 h of cycling. Coulombic efficiencies of >99.96% were observed; again these results are consistent with stripping and plating rather than processes dominated by electrolyte decomposition.

Visual inspection and scanning electron microscopy (SEM) images of ss-316 current collectors extracted after 30 min charge/discharge steps for ~250 cycles show large discolored areas on the surface of the material, features that are not present on pristine ss-316 current collectors (Figures 3b–e), suggesting that some corrosion or electrolyte breakdown has occurred during cycling. SEM images of the Mg metal taken from these cycled cells show the presence of globular masses that are composed almost exclusively of Mg and which are not present on the as-prepared Mg electrodes (Figure 4b,d); these Mg globules on the majority of the Mg surface are a clear indication of Mg plating.[5b,15] Further, energy-dispersive X-ray spectroscopy (EDX) measurements and element mapping conducted on these large areas of plated Mg exhibit little to no evidence of fluorine being present on the surface, contradicting established thought regarding the formation of passivating fluoride-rich films on Mg (Figures S14–S17). Compared to the as-prepared Mg electrodes, the cycled material shows only slightly increased amounts of O, and element mapping demonstrates that O is not homogeneously distributed over the surface but isolated to specific regions and could arise from THF decomposition or air exposure during SEM sample preparation (Figures S13–S17). While EDX does not conclusively identify the nature of the corrosion or electrolyte breakdown on the surface of the ss-316 current collectors, small areas of the cycled Mg electrodes exhibit traces of Fe and Cr, which were likely deposited as a result of ss-316 corrosion (Figure S20).

SEM images and EDX measurements conducted on Al current collectors taken from a cycled Mg symmetric cell (cycled in the same manner as the ss-316 cell, above; Figure S10) show much less evidence of corrosion or electrolyte decomposition on the Al surface (Figures S21–S24). There are a few isolated areas that display pits in the surface that are rich in F, O, and Fe when compared to neighboring areas as well as the pristine material, possibly resulting from minor reactivity with the electrolyte and corrosion of the ss-316 cell casing during cycling. Again, the Mg electrodes extracted from this cell showed surface morphologies similar to those taken from the ss-316 cell by SEM—a surface patterned with Mg globules, confirming the Mg plating in the cell (Figure 4c,e–g).

Having demonstrated plating and stripping of Mg, we used the 0.71 M electrolyte solution in coin cells constructed using a Mg anode, and a Chevrel (Mo_3S_4)-phase cathode. Owing to the observed stability of this electrolyte on Al, current collectors made of Al were employed to limit possible side reactions during battery cycling. The coin cells, cycled at C/100, showed reversible charge/discharge profiles and could be cycled for at least five cycles, reaching a maximum reversible capacity of 51 mAh·g^{-1}, roughly half of the theoretical capacity (Figure 5). We note that the measured voltages associated with the two characteristic processes for Mg insertion and removal from the

DOI: 10.1021/jacs.6b04319
J. Am. Chem. Soc. 2016, 138, 8682–8685

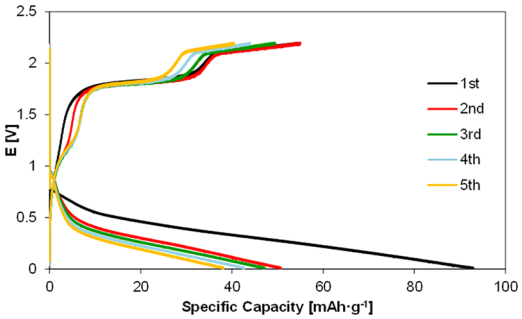

Figure 5. Five galvanostatic discharge/charge cycles of a coin cell containing a 0.71 M solution of **1** in 1:1 THF/CH_3CN, a Mg anode, an Mo_3S_4 cathode, and Al current collectors, cycling at a rate of C/100.

Chevrel phase are associated with overpotentials of >0.4 V, which are likely due to kinetic limitations of both stripping/plating and insertion/removal of Mg^{2+} ions at the positive and negative electrodes, respectively. The observed capacity is similar to that observed for the $LiBH_4/Mg(BH_4)_2$/DME electrolyte (albeit with higher overpotentials),[16] but worse than that observed in Al- or B-based electrolytes.[5a,17] More work is required to explore the role of other solvents beyond THF to lower the overpotential for intercalation and the use of these electrolytes with other positive electrode materials.

In summary, we synthesized the first $Mg(PF_6)_2$ complex (**1**), providing access to a group 2 complex containing labile CH_3CN ligands and weakly coordinating anions that could be used as a general precursor for the formation of alkaline earth metal catalysts or as a reagent itself.[18] Further, we demonstrated successful plating and stripping of Mg from a $Mg(PF_6)_2$-based electrolyte system. These $Mg(PF_6)_2$-based electrolytes exhibit a large stability window on Al (>4.0 V vs Mg) and can be cycled on Mg without any noticeable loss in electrochemical activity of the Mg electrode. LSV and EDX studies show that these electrolytes react with stainless steel electrodes, resulting in corrosion of the electrode surface. Contrary to expectations, SEM and EDX measurements of Mg electrodes taken from cycled symmetric cells show that Mg is plated from $Mg(PF_6)_2$ solutions and that the surface remains electrochemically active after multiple voltammetric cycles, as no passivating MgF_2 films are observed to form on the surface of the cycled Mg electrode. Lastly, 0.71 M electrolyte solutions of **1** in 1:1 THF/CH_3CN have been shown to allow the reversible cycling of a coin cell containing a Mg anode, a Chevrel-phase cathode, and Al current collectors with a maximum reversible capacity of 51 $mAh{\cdot}g^{-1}$; studies involving the use of this electrolyte with other positive electrodes are in progress. We are continuing to study the electrochemistry and ionic conductivity of $Mg(PF_6)_2$-based electrolytes with different solvents to gain a more thorough understanding of the solution-state structure of the $Mg(PF_6)_2$ salt, its effect on the stability of the electrolyte solution, and its possible role as an additive in other electrolytes for the passivation of current collectors.[19]

■ ASSOCIATED CONTENT

Supporting Information

The Supporting Information is available free of charge on the ACS Publications website at DOI: 10.1021/jacs.6b04319.

X-ray crystallographic data for **1** (CIF)
Experimental details, spectra, supporting Figures S1−S24, and crystallographic details for **1** (PDF)

■ AUTHOR INFORMATION

Corresponding Authors

*cpg27@cam.ac.uk
*dsw1000@cam.ac.uk

Notes

The authors declare no competing financial interest.

■ ACKNOWLEDGMENTS

E.N.K. thanks NSERC for a PGS D as well as the Cambridge Commonwealth, European, and International Trust and Gonville and Caius College for funding. This work was supported by the EPSRC Cambridge NanoDTC, EP/G037221/1. The authors thank William J. Ramsey for helpful discussions and Andrew D. Bond and Peter D. Matthews for their contributions to crystal structure refinement.

■ REFERENCES

(1) (a) Armand, M.; Tarascon, J.-M. *Nature* **2008**, *451*, 652. (b) Van Noorden, R. *Nature* **2014**, *507*, 26.
(2) Muldoon, J.; Bucur, C. B.; Gregory, T. *Chem. Rev.* **2014**, *114*, 11683.
(3) Wen, J.; Yu, Y.; Chen, C. *Mater. Express* **2012**, *2*, 197.
(4) Muldoon, J.; Bucur, C. B.; Oliver, A. G.; Sugimoto, T.; Matsui, M.; Kim, H. S.; Allred, G. D.; Zajicek, J.; Kotani, Y. *Energy Environ. Sci.* **2012**, *5*, 5941.
(5) (a) Liu, T.; Shao, Y.; Li, G.; Gu, M.; Hu, J.; Xu, S.; Nie, Z.; Chen, X.; Wang, C.; Liu, J. *J. Mater. Chem. A* **2014**, *2*, 3430. (b) Ha, S.; Lee, Y.; Woo, S. W.; Koo, B.; Kim, J.; Cho, J.; Lee, K. T.; Choi, N. *ACS Appl. Mater. Interfaces* **2014**, *6*, 4063.
(6) (a) Xu, K. *Chem. Rev.* **2004**, *104*, 4303. (b) Etacheri, V.; Marom, R.; Elazari, R.; Salitra, G.; Aurbach, D. *Energy Environ. Sci.* **2011**, *4*, 3243.
(7) Ozawa, K. *Solid State Ionics* **1994**, *69*, 212.
(8) (a) Guyomard, D.; Tarascon, J. M. *Solid State Ionics* **1994**, *69*, 222. (b) Ue, M.; Takeda, M.; Masahiro, T.; Mori, S. *J. Electrochem. Soc.* **1997**, *144*, 2684.
(9) Markovsky, B.; Amalraj, F.; Gottlieb, H. E.; Gofer, Y.; Martha, S. K.; Aurbach, D. *J. Electrochem. Soc.* **2010**, *157*, A423.
(10) (a) Lu, Z.; Schechter, A.; Moshkovich, M.; Aurbach, D. *J. Electroanal. Chem.* **1999**, *466*, 203. (b) Muldoon, J.; Bucur, C. B.; Oliver, A. G.; Zajicek, J.; Allred, G. D.; Boggess, W. C. *Energy Environ. Sci.* **2013**, *6*, 482.
(11) Lipson, A. L.; Pan, B.; Lapidus, S. H.; Liao, C.; Vaughey, J. T.; Ingram, B. J. *Chem. Mater.* **2015**, *27*, 8442.
(12) Haiges, R.; Christe, K. O. *Z. Anorg. Allg. Chem.* **2002**, *628*, 1717.
(13) (a) Heintz, R. A.; Smith, J. A.; Szalay, P. S.; Weisgerber, A.; Dunbar, K. R. In *Inorganic Syntheses*; Beck, K., Coucouvanis, D., Eds.; Wiley: New York, 2002; Vol. 33, pp 75−121. (b) Clegg, J. K.; Cremers, J.; Hogben, A. J.; Breiner, B.; Smulders, M. M. J.; Thoburn, J. D.; Nitschke, J. R. *Chem. Sci.* **2013**, *4*, 68.
(14) (a) Laoire, C. O.; Mukerjee, S.; Abraham, K. M.; Plichta, E. J.; Hendrickson, M. a. *J. Phys. Chem. C* **2010**, *114*, 9178. (b) Seo, D. M.; Borodin, O.; Balogh, D.; O'Connell, M.; Ly, Q.; Han, S.-D.; Passerini, S.; Henderson, W. A. *J. Electrochem. Soc.* **2013**, *160*, A1061.
(15) Matsui, M. *J. Power Sources* **2011**, *196*, 7048.
(16) Mohtadi, R.; Matsui, M.; Arthur, T. S.; Hwang, S. J. *Angew. Chem., Int. Ed.* **2012**, *51* (39), 9780.
(17) (a) Aurbach, D.; Lu, Z.; Schechter, A.; Gofer, Y.; Gizbar, H.; Turgeman, R.; Cohen, Y.; Moshkovich, M.; Levi, E. *Nature* **2000**, *407* (6805), 724. (b) Doe, R. E.; Han, R.; Hwang, J.; Gmitter, A. J.; Shterenberg, I.; Yoo, H. D.; Pour, N.; Aurbach, D. *Chem. Commun.* **2014**, *50*, 243. (c) Guo, Y.; Zhang, F.; Yang, J.; Wang, F.; NuLi, Y.; Hirano, S. *Energy Environ. Sci.* **2012**, *5*, 9100.
(18) (a) Rochat, R.; Lopez, M. J.; Tsurugi, H.; Mashima, K. *ChemCatChem* **2016**, *8*, 10. (b) Hill, M. S.; Liptrot, D. J.; Weetman, C. *Chem. Soc. Rev.* **2016**, *45*, 972.
(19) Wang, X.; Yasukawa, E.; Mori, S. *Electrochim. Acta* **2000**, *45*, 2677.

DOI: 10.1021/jacs.6b04319
J. Am. Chem. Soc. 2016, 138, 8682−8685